A&A 639, A5 (2020)
https://doi.org/10.1051/0004-6361/202038014

Astronomy & Astrophysics

X-ray absorption in INTEGRAL active galactic nuclei

Host galaxy inclination*

A. Malizia[1], L. Bassani[1], J. B. Stephen[1], A. Bazzano[2], and P. Ubertini[2]

[1] Osservatorio di Astrofisica Spaziale e Scienza dello Spazio – INAF, Via P. Gobetti 101, 40129 Bologna, Italy
e-mail: angela.malizia@inaf.it
[2] Istituto di Astrofisica e Planetologia Spaziali – INAF, Via Fosso del Cavaliere 100, 00133 Roma, Italy

Received 24 March 2020 / Accepted 29 April 2020

ABSTRACT

In this work the INTEGRAL hard X-ray selected sample of active galactic nuclei (AGN) has been used to investigate the possible contribution of absorbing material distributed within the host galaxies to the total amount of $N_{\rm H}$ measured in the X-ray band. We collected all the available axial ratio measurements of the galaxies hosting our AGN together with their morphological information and found that for our hard X-ray selected sample as well there is a deficit of edge-on galaxies hosting type 1 AGN. We estimate that in our hard X-ray selected sample there is a deficit of 24% (±5%) of type 1 AGN. Possible bias in redshift has been excluded, as we found the same effect in a well-determined range of z where the number and the distributions of the two classes are statistically the same. Our findings clearly indicate that material located in the host galaxy on scales of hundreds of parsecs and not aligned with the putative absorbing torus of the AGN can contribute to the total amount of column density. This galactic absorber could be large enough to hide the broad line region of some type 1 AGN, thus causing their classification as type 2 objects and giving rise to the deficiency of type 1 objects in edge-on galaxies.

Key words. X-rays: galaxies – galaxies: active – galaxies: Seyfert

1. Introduction

The nature of the absorbing material that hides the central engine of active galactic nuclei (AGN) is crucial to our understanding of the physics of these objects (Hickox & Alexander 2018). It is also a key issue in the unified model of AGN (Antonucci 1993; Urry & Padovani 1995), which in its simplest version postulates that the diversity of AGN can be largely explained as a viewing angle effect. The most important ingredient in this orientation-based model is an optically and geometrically thick torus that obscures the nuclear regions of an active galaxy (the accretion disc and the hot corona as well as the broad line region (BLR)). We optically classify an AGN as type 2 or type 1 depending on whether our line of sight intercepts the obscuring material of the torus or not.

The validity of the unified model of AGN has largely been tested and confirmed by the presence of high absorption measured in the X-ray spectra of type 2 with respect to lower amounts found in type 1 AGN. In particular, using a sample of 272 AGN observed at high energies (>20 keV) by INTEGRAL/IBIS we have found that the standard-based AGN unification scheme is followed by the majority of bright AGN (Malizia et al. 2012) with only a few exceptions related to 12−13% of the objects. These exceptions are absorbed type 1 and unabsorbed type 2 AGN. The absorption in type 1 AGN is generally interpreted in terms of ionised gas located in an accretion disc wind or in the biconical structure associated with the central nucleus and therefore unrelated to the torus. The lack of X-ray absorption ($N_{\rm H} < 10^{22}$ cm^{-2}) in type 2 AGN could be explained by the assumption that the torus is either not present (or has disappeared) or the source has been misclassified. The first case is probably true for low luminosity objects (Elitzur 2008) while the second case is relevant for the class of intermediate type 2 Seyfert (type 1.8−1.9). These intermediate objects have historically been considered as AGN where the observer's line of sight intercepts either the outer edge of the torus or a limited number of clouds, so that the broad line region is still partly visible. However, in Malizia et al. (2012) we also pointed out that these intermediate classifications can be explained by an intrinsically variable ionising continuum or by the presence of absorption/reddening unrelated to the torus. For example, a source that would normally appear as a type 1 Seyfert can be classified as an intermediate type if it is in a low optical flux state (Trippe et al. 2010) or if its BLR is obscured (except for the strongest H_α line) by dust related to large-scale structures such as bars, dust lanes, and host galaxy material (Malkan et al. 1998; Matt 2000).

Thus absorption in AGN is probably due not only to one component, the torus, but to multiple components on very different scales. Bianchi et al. (2012) identified three such components: the BLR on the 0.01 pc scale, the torus on a parsec scale, and absorption located in the host galaxy on a scale of hundreds of parsecs.

Evidence for large-scale absorption comes mostly from inclination studies of the host galaxies of AGN. In one of the first such studies, Keel (1980) found that optically selected (mostly type 1) Seyferts tend to avoid edge-on host galaxies. Using a sample of AGN selected in the soft X-ray band (0.2−3.5 keV), Simcoe et al. (1997) subsequently confirmed the bias against

* Tables A1–A3 are only available at the CDS via anonymous ftp to cdsarc.u-strasbg.fr (130.79.128.5) or via http://cdsarc.u-strasbg.fr/viz-bin/cat/J/A+A/639/A5

edge-on Seyfert 1, although they were able to recover some of the edge-on AGN missed in UV and visible surveys, resulting in 30% incompleteness for type 1's. However, since the soft X-ray band can also be biased in terms of absorption, a definitive test would be provided by the use of a hard X-ray selected sample. A preliminary analysis performed on a *Swift*/Burst Alert Telescope (BAT) sample of around 80 AGN by Winter et al. (2009) showed that objects with low X-ray column densities were preferentially found in galaxies with low inclination angles (face-on, $b/a > 0.5$), while those with higher column densities were found in galaxies of any inclination (edge-on and face-on, $0.1 < b/a < 1$). The finding that optically selected AGN samples tend to avoid edge-on systems has recently been confirmed and refined with much higher statistics by using the Sloan Digital Sky Survey (Lagos et al. 2011).

The first explanations for this result came from Maiolino & Rieke (1995) and Matt (2000). Maiolino & Rieke (1995) proposed the dual absorber model, which foresees the existence of an obscuring material of molecular gas on a scale of 100 pc that is coplanar with the galactic disc and not necessarily aligned with the torus. On the other hand, taking into account observational evidence, Matt (2000) proposed a scenario where Compton thick Seyfert 2 galaxies are those sources observed through the torus, while Compton thin and intermediate Seyfert galaxies are obscured by dust lanes at larger distances.

Focusing on the possible origin of the galactic absorber, a major study is that of Malkan et al. (1998), who detected fine-scale structure in the centres of nearby galaxies using *Hubble* Space Telescope images: these structures include dust lanes and patches, bars, rings, wisps, filaments, and tidal features such as warps and tails. These authors even suggested a new unified model (the galactic dust model) whereby the obscuration that converts an intrinsic Seyfert 1 nucleus into an apparent Seyfert 2 occurs in the host galaxy hundreds of parsecs from the nucleus. More recently Prieto et al. (2014) confirmed these early results, demonstrating the existence of large-scale (a few hundred parsecs) dust filaments and diffuse dust lanes that hide the central region of some AGN.

Nowadays the parsec-scale environment of AGN can be spatially resolved by high angular resolution observations in the infrared (IR) with VLTI and in the sub-millimetre by Atacama Large Millimeter/submillimeter Array (ALMA) (see e.g. Hönig & Kishimoto 2017; Combes et al. 2019), which draws a much more complex picture of multi-phase and multi-component regions. Recently Hönig (2019) has proposed a model that accounts for these new observations wherein dusty molecular gas flows in from the host galaxy (~100 pc) to the sub-parsec environment via a disc of small to moderate height. Due to the radiation pressure, the disc puffs up and unbinds a large amount of the inflowing gas from the black hole's gravitational potential allowing the creation of dusty molecular winds driven by the radiation pressure from the AGN. These dusty winds feed back into the host galaxy with a rate that increases with the AGN luminosity (or Eddington ratio), and are therefore a mechanism to self-regulate the AGN activity, providing a feedback from AGN to host galaxy. Within this picture there are multiple spatial and dynamical components that obscure the primary emission rather than a single torus. For local, radio-quiet, active galaxies, Hoenig's model is consistent with the structure proposed by Ricci et al. (2017) to explain the X-ray obscuration in AGN. ALMA observations have revealed the presence of circumnuclear molecular (CO) gas in many Seyfert galaxies (Schinnerer et al. 1999), as well as the presence of cold gas and dust at scales of hundreds of parsecs in many AGN host galaxies (e.g. García-Burillo et al. 2005, 2014).

Finally, we note that large-scale absorption may come also from non-asymmetric perturbations that provide a viable way to channel gas from the outer part of a galaxy into its central regions. These perturbations can be of two types: external, such as galaxy-galaxy interactions, or internal, such as due to bars and their gravity torques. Observations indicate that an AGN becomes heavily obscured behind merger-driven gas and dust, even in the early stages of galaxy-galaxy interaction, when the galaxies are still well separated (Kocevski et al. 2015). Furthermore, analysis of *Swift*/BAT AGN indicates that a large fraction (25%) of these objects show disturbed morphologies or are in close physical pairs compared to matched control galaxies or optically selected AGN (Koss et al. 2010).

In this paper we investigate the presence and role of obscuration on large galactic scales and its relation with the X-ray column density, by examining the axial ratio distribution in a well-defined sample of INTEGRAL selected AGN, listed in Malizia et al. (2012, 2016) and newly reported in this work. This sample, being hard X-ray selected, is the most appropriate to carry out this type of study since it is unbiased against obscured objects and therefore free of the limitation that affects surveys at other frequencies (i.e. from optical to soft X-rays).

2. Sample

In order to have a well-defined hard X-ray selected sample of AGN, we considered all the INTEGRAL Seyferts listed in Malizia et al. (2012, 2016) plus those reported in Tables A.2 and A.3. This hard X-ray selected sample of AGN has been extracted from the INTEGRAL/IBIS all sky surveys performed so far in the 20−100 keV band (Bird et al. 2016, and reference therein). This sample has been updated in this work with the addition of the new AGN reported by Mereminskiy et al. (2016) in the deep extragalactic surveys of M 81, LMC and 3C 273/Coma regions, and those reported by Krivonos et al. (2017) in the Galactic Plane Survey (see Tables A.2 and A.3 for details on these new additions).

The entire INTEGRAL AGN sample is fully characterised in terms of optical identification and classification and is also fully studied in terms of X-ray spectral properties (see Malizia et al. 2012). In particular, the column densities ($N_{\rm H}$) measured in the 2−10 keV band for each AGN have been collected from the literature (see Malizia et al. 2012, 2016) or calculated for the newly added sources in this work (see Tables A.2 and A.3). All together, we have gathered a sample of 376 hard X-ray selected active galaxies, with a well defined set of information. Objects identified as blazars in the IBIS surveys have been excluded from the analysis to avoid complication due to the presence of jets pointing towards the observer. Following our previous works we divided our AGN into type 1, comprising all the broad line Seyferts of our sample and including Seyfert 1, 1.2, and 1.5 (179 objects), and type 2 objects comprising all the narrow line AGN, that is, Seyfert 1.8, 1.9, and 2 (197 objects). Twenty-two objects (~6% of the sample) have an unknown optical classification or belong to non-Seyfert optical classes (low-ionisation nuclear emission-line region (liners), XBONG, AGN), therefore they have been assimilated into type 1 or 2 AGN depending on whether they were absorbed (21 objects) or not in the X-ray band. Performing the complete analysis without these sources does not significantly change the overall results.

In order to investigate the role of absorption in the host galaxy, for the entire sample we collected the axial ratio b/a,

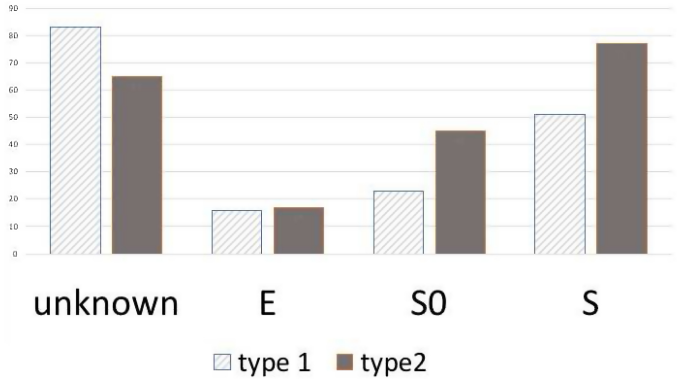

Fig. 1. Histogram of the morphological classification following the de Vaucouleurs (1959) scheme. Unknown: galaxies which have no host galaxy morphology; E: elliptical galaxies; S0: intermediate systems between ellipticals and spirals; S: spiral galaxies. Objects are further sub-divided into type 1 and type 2.

used here as a proxy for the host galaxy inclination (to first order, cos $i = b/a$ where a and b are the observed major and minor axes of a galaxy and i is its inclination). These values have been collected from the Two Micron All Sky Survey (2MASS)[1], where information was available for 300 objects out of 376 in the sample (i.e. the largest coverage available in catalogues with b/a information) and they are reported in Cols. 5 and 10 of Tables A.1–A.3 respectively. It is worth noting that as described by Jarrett et al. (2003), the 2MASS images, co-adding J, H, and K bands, have a point spread function full width at half maximum (FWHM) of 2−3 arcsec. This value is much smaller that the radii of our galaxies (around 20−30 arcsec or more) collected from the same archive, therefore excluding any possible bias in the b/a measurements used in our work, especially for type 1 objects hosting a bright nucleus. Furthermore, in order to verify the accuracy of these axial ratios, we used the Pan-STARRS1 database (Chambers et al. 2016) and extracted the DR1 colour (g to z filter) images for a representative sample of over 30 of our objects ranging in axial ratio from 0.1 to 0.9 and over all optical classes. A representative set of objects amongst those with no optical classification was also checked. We then fitted ellipses to these images in order to measure their axial ratio values. In every case these values were consistent with those extracted from the 2MASS surveys and used originally.

3. Absorption and source morphology

Indications that absorption on a galaxy scale is important in the overall column density budget of an AGN, suggests a possible link between galaxy morphology and $N_{\rm H}$. We have therefore collected data for both these two parameters. Data for host galaxy morphological information for all objects come from the Hyperleda catalogue (Makarov et al. 2014), the NASA/IPAC Extragalactic Database (NED) archive and the 2MASS Redshift Survey (Huchra et al. 2012): the most quoted classification amongst these three databases has been adopted and reported in Tables A1–A3. When no information or different classification were available, we have also searched the literature for extra information (Maiolino et al. 1999; Madrid et al. 2006; McKernan et al. 2010; Maia et al. 2003; Tsvetanov et al. 1992; Ferruit et al. 2000). Data for $N_{\rm H}$ values come instead from our previous publications and current paper as specified in Sect. 2.

[1] http://irsa.ipac.caltech.edu/cgi-bin/Gator/nph-dd

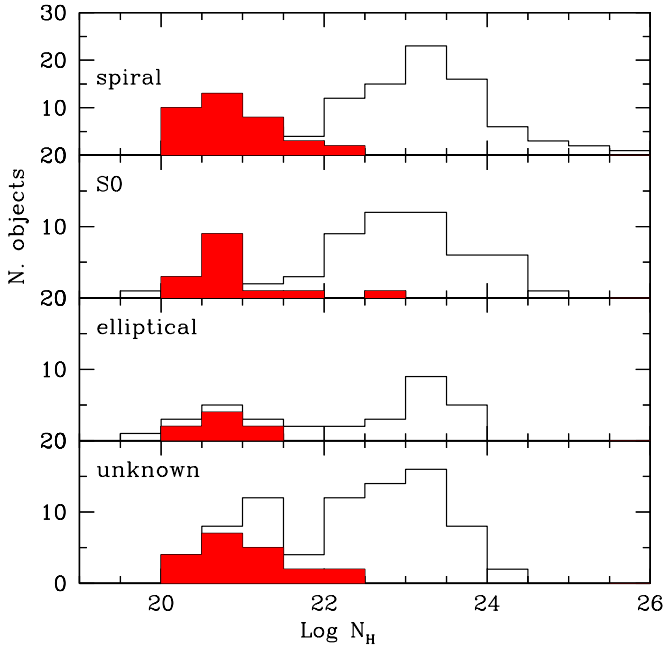

Fig. 2. Distribution of column density in each morphological class; X-ray absorption in AGN hosted in galaxies of unknown class is also shown. Filled red bins refer to Galactic or upper limit values of $N_{\rm H}$.

All the INTEGRAL AGN have been divided into three broad morphological types following the de Vaucouleurs (1959) scheme: E to describe elliptical galaxies, S0 for objects which are intermediate systems between ellipticals and spirals (alternatively called lenticular galaxies), and S for spiral galaxies. The distribution of INTEGRAL AGN in each morphological class, including those objects for which the host galaxy morphology is unknown, is shown in Fig. 1, where the predominance of spiral and lenticular galaxies over ellipticals is evident. The greater number of type 2 over type 1 AGN in both S0 and S classes is also clear.

We have been able to obtain morphological host galaxy information for 228 objects or 61% of the sample. This low fraction is due to the fact that many INTEGRAL AGN are newly discovered galaxies, often located on the Galactic Plane, which is in the zone of avoidance, and therefore their morphology is still poorly studied. In the nearby Universe, elliptical galaxies are known to have less gas, dust, and ongoing star formation activity than spiral galaxies (Hirashita & Nozawa 2017, and references therein). Figure 2 shows the histogram of each morphological class as a function of X-ray column density: while there seems to be no difference in absorption properties between different classes for column density below Log$N_{\rm H} = 24$, some difference is evident above, since no Compton thick AGN is hosted in an elliptical host galaxy. However, this may be due to low number statistic, given the limited number of ellipticals considered here, as they count for only 14% of the entire INTEGRAL AGN sample. The fraction of heavily absorbed AGN is around 11% for both spiral and lenticular galaxies; if the same fraction is applied to ellipticals, then we would expect three to four objects in this class to be Compton thick, while none are observed.

The evidence of a lower fraction of Compton thick AGN in hard X-ray radio galaxies, typically hosted in elliptical galaxies, has already been discussed by Panessa et al. (2016) and Ursini et al. (2017) and is definitely an issue that deserves further investigation. Ursini et al. (2017) also noted that a significant

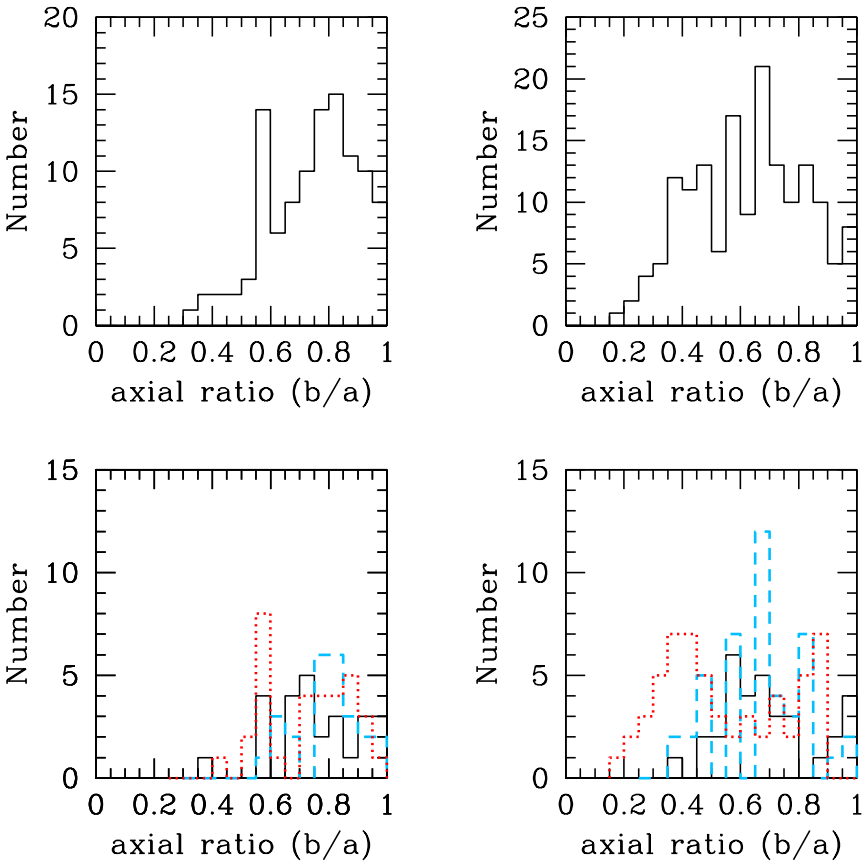

Fig. 3. Distribution of host galaxy axial ratios of INTEGRAL AGN differentiated into broad lines or type 1 i.e. Sy 1−1.2−1.5 (*upper and lower left panels*), and narrow lines or type 2 i.e. Sy 1.8−1.9−2 (*upper and lower right panels*). *Lower panels*: the morphological type of our sample sources has been considered; histograms in dotted red lines refer to AGN hosted in late type (spirals) galaxies, blue dashed lines refer to AGN hosted in early (elliptical and S0) galaxies, and black solid lines refer to host galaxies for which no morphological type has been found in the literature.

role in the absorption of heavily absorbed radio galaxies could be played by material different from the classical parsec-scale torus, such as that traced by 21 cm H_I absorption, which can be located much farther away, for example at galactic scales. Therefore observational evidence even questions the origin of the X-ray absorption in ellipticals and hints at a possible difference between the average properties of ellipticals compared to lenticular and spiral galaxies, especially in terms of Compton thick absorption.

4. Inclination of host galaxies

Using the large INTEGRAL AGN sample, in this section we explore the axial ratio distribution of broad and narrow line AGN: Fig. 3 displays the histograms of b/a by galaxy type and within each type divided in morphological classes. The lack of galaxies with $b/a < 0.2$ is due to the non-zero thickness of the disc, which accounts for the fact that, even when seen edge-on, a galaxy has b/a greater than zero (Hubble 1926). Amongst the 122 type 1 AGN of our sample for which we obtained axial ratio information, only 12 (<10%) have a host galaxy axial ratio below 0.5; this percentage is much higher in type 2 AGN where 50 out of 178 type 2 objects (or 28%) have $b/a < 0.5$[2]. By performing a Kolmogorov–Smirnov (KS) test, we find that the axial ratio distributions of type 1 and type 2 AGN are different, since the probability that the two samples come from the same distribution is rejected at a confidence level of 99.99%. In order to quantify the deficit of type 1 AGN at low inclination angles, we compare the two histogram distributions. Taking the difference between the two histograms, and assuming that above an inclination angle of 0.5 they are from identical distributions, we normalise it so that the total difference in number of sources above that value is zero. In order to have a difference of zero below that threshold, 38 ± 11 sources must be missing from the type 1 distribution. This implies that in this sample there is a deficit of about 24% (±5%) of type 1 AGN, in agreement with Simcoe et al. (1997) who found 30% for an X-ray selected sample.

Furthermore, using the information on the host galaxies' morphology and dividing the objects into early (ellipticals and S0) and late (spirals) types, we also checked if the bias against edge-on host galaxies of broad line AGN is related to any specific morphological type or is present in both types. Using (here and in the following) a confidence level of 99% and applying the KS test, we find that the two distributions (type 1 versus type 2 AGN) are different both for early type as well as late type objects. This is also evident in Fig. 3 where the different morphology types have been highlighted for type 1 and 2 AGN respectively. We therefore confirm that, even using AGN selected above 20 keV, the deficit of type 1 AGN hosted in edge-on galaxies exists in, and is independent of, all morphological types.

In addition to this deficit, it is interesting that type 2 AGN are distributed over the whole range of b/a. This result confirms previous findings but also highlights the fact that this lack of Seyfert 1 in edge-on galaxies is not due to observational bias. As pointed out by Gelbord et al. (2006), if the torus was the only obscuration matter, then two possible scenarios should be taken into consideration: the first where the torus and the host galaxy plane are aligned and the second where the two are misaligned. In the first case we should see a distribution of type 1 Seyferts that peaks in face-on galaxies and a distribution of type 2 Seyferts

[2] It is worth noting that the absorbed sources with no optical class considered as type 2 have axial ratio distributed over the whole range of b/a, and the only unclassified source included in the type 1 class has $b/a = 0.58$.

that peaks in edge-on galaxies, while in the second case no correlation between Seyfert type and host galaxy inclination would be expected. From the studies performed so far and confirmed herein, neither of these two scenarios are compatible with the observational evidence since broad line AGN have a strong correlation with the host inclination angle while type 2 AGN are broadly distributed over the whole b/a range. Our findings indicate that something intervenes outside the nucleus of the AGN (on hundreds of parsecs scales), likely in the host galaxy; this absorbing material, which might not be aligned with the torus, can contribute to the final column density measured in the X-ray band.

From recent ALMA observations of some AGN, we have an indication that the molecular discs, or tori, detected at 10 pc scales are kinematically decoupled from their host galaxy disc and have random orientations (Combes et al. 2019). Assuming a simplistic approach, which does not consider the BLR but only the host galaxy and the torus, we expect the following four configurations depending on their relative alignment or misalignment. If the torus is edge-on, the source is always classified as a type 2 AGN and should present X-ray absorption, whether or not the galaxy is seen edge-on or face-on. If the torus is seen face-on, then we should expect a type 1 AGN configuration with no or very mild absorption unless the galaxy is seen edge-on and has absorbing material on a large scale. In this last case the source could be wrongly classified as a type 2 AGN although the absorption is not related to the torus. This is schematically shown in Fig. 4 where the horizontal line represents the dividing line between face-on and edge-on host galaxies at $b/a = 0.5$, while the first vertical line represents instead the value of $N_{\rm H} = 4 \times 10^{21}$ cm^{-2} , which has been assumed as the dividing line between absorbed and unabsorbed objects. This value has been taken from Mateos et al. (2016) and corresponds to the extinction level capable of hiding the BLR. The dashed region delimited by Log$N_{\rm H} \leq 23$ and $b/a \leq 0.5$, represents the area where misclassified type 1 AGN could be located (i.e. galaxy absorption in an edge-on host is sufficient to hide the broad line region). With this scheme in mind, we can now investigate the relation between host galaxy inclination and X-ray absorption.

Before drawing any further conclusions from the observed axial ratio distribution, any possible bias introduced by the sample redshift distribution must be checked. It is important to investigate this issue since there are two considerations that pertain to the use of a non-complete sample of AGN. The first is that at high redshifts, the sources become point-like and therefore it is very difficult to estimate the host galaxy axial ratio. The second concerns the widely known fact that in the local Universe type 2 objects outnumber type 1 sources by a factor of ∼4 and more (Sazonov et al. 2015); whether this effect can be explained by cosmological reasons or not is still a matter of debate. These two effects are highlighted in Fig. 5 where it is clear that the distributions of type 1 and type 2 galaxies are different in the z–b/a plane: there are considerably more type 2 AGN at low z values than type 1 and very few objects at high redshifts have axial ratio measurements. In order to minimise these effects, we decided to analyse a subset of the two AGN populations restricting both high and low z values. To do this, we first choose all sources between a lower and higher limit of redshift. The distribution of type 1 and type 2 objects between these two limits is then compared and the KS statistic applied to identify if they come from the same population. This is done for all possible combinations of the two limits in z. The combination that provides the highest probability that the two populations come from the same z distribution (at 99.9% confidence) are then further reduced to give

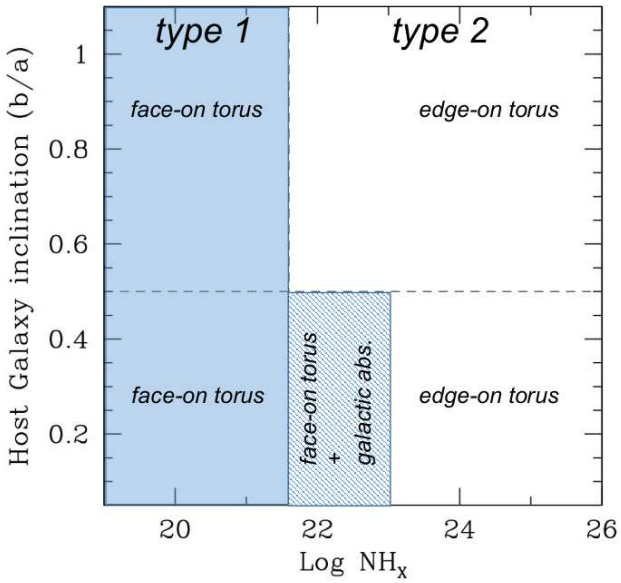

Fig. 4. Scheme of the expected type of absorption in the b/a–$N_{\rm H}$ plane for broad line (left blue side) and narrow line AGN (right side) in relation to the torus and host galaxy misalignment. The dashed blue region represents values where a type 1 AGN could be likely classified as type 2 due to absorption located in the host galaxy.

the largest total number of objects. In this manner, we found that allowing the redshift to range from 0.026 to 0.095, we obtained a total number of 133 AGN with z within this range; of these AGN, 66 are of type 1 and 67 of type 2, with a probability of 99.97% that they come from the same overall redshift distribution (top panels of Fig. 6). Next, the distribution of the axial ratio of these 133 sources divided in two optical classes were compared as shown in Fig. 6 (lower panels). Again the two distributions are found to be different, with type 1 objects mainly located in face-on galaxies and type 2 spread over the entire range of b/a values. Using the KS statistic we find that the likelihood that the two populations come from the same distribution is rejected at a confidence level of 99.75% implying that no bias in redshift affects our result.

5. Host galaxy inclination versus X-ray absorption

In order to investigate the deficit of type 1 AGN in edge-on galaxies in more detail, we first considered for each AGN type their optical sub-classes, which is a way to investigate if and how the broad line region is detected. In Fig. 7 panel a, we compare the axial ratio distribution of Seyfert 1−1.2 (solid black line) and Seyfert 1.5 (dashed red line). As is evident in the figure but also quantified by the KS test, the two distributions are similar (at a confidence level of 99%) indicating that the deficit of broad line AGN in edge-on galaxies is present in all subclasses.

Equally, in panel b of Fig. 7, the distribution of axial ratios in Seyfert 2 (black solid line) and Seyfert 1.8−1.9 (blue dashed line) are plotted in order to see if they are distributed differently and, as is clear from the histograms and quantified by the KS statistics, they are not. Also including all the sources of intermediate class (1.2, 1.5, 1.8 and 1.9) in the type 1 sample and leaving in the type 2 only the pure Seyfert 2 objects, the two distributions were statistically different. The same result has been found considering only the high energy selected AGN belonging to the INTEGRAL complete sample (Malizia et al. 2009).

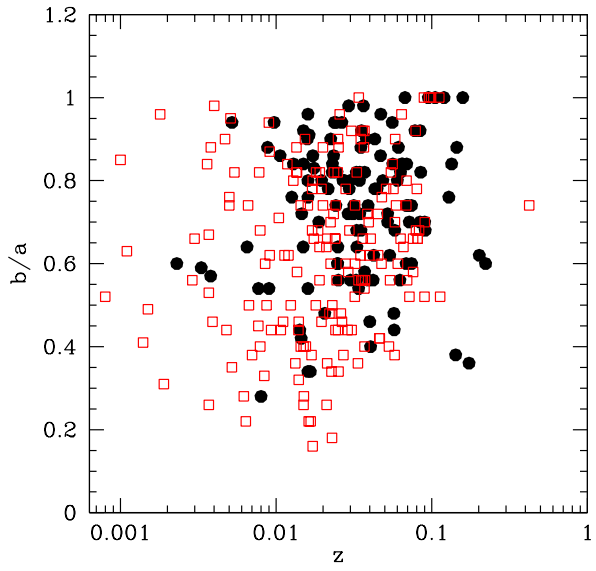

Fig. 5. Redshift values of the INTEGRAL AGN plotted against the axial ratios of their host galaxies. Filled black circles are type 1 AGN while open red squares are type 2.

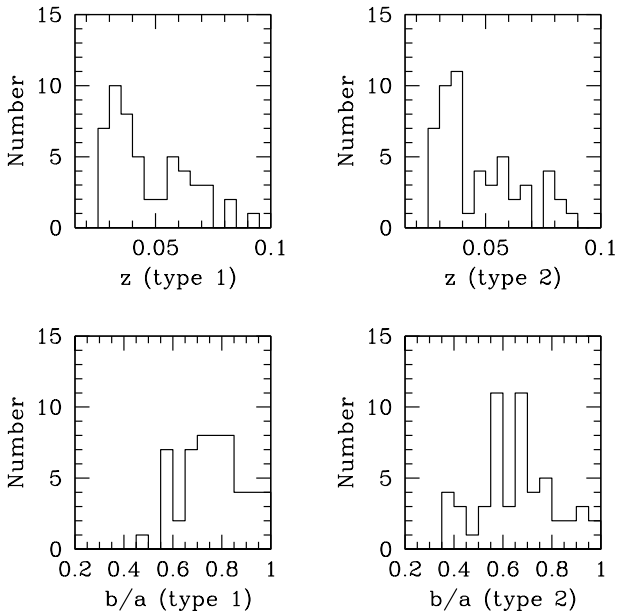

Fig. 6. Distributions of redshift values in type 1 (*left*) and type 2 (*right*) AGN in the bins 0.026 and 0.095 (*upper panels*) and distributions of their relative axial ratios (*bottom panels*).

In Fig. 7 panel c we plot the axial ratios of type 1 AGN (Seyfert 1−1.2 black circles and Seyfert 1.5 red circles) versus the X-ray absorption; the open circles indicate no intrinsic absorption (i.e. only Galactic) or upper limits. Note that in panels c and d of Fig. 7 the horizontal and vertical dashed lines follow the scheme introduced in Fig. 4.

As expected from the scheme of Fig. 4, type 1 AGN fall mostly in the top left side of panel c, thus corresponding to the situation where the torus and the galaxy are both seen face-on and no or mild X-ray absorption is present. Regarding those type 1 AGN which, despite having torus and galaxy both face-on display X-ray absorption (i.e. fall in the upper right side of panel c), we assume that they can be largely explained as objects where the absorbing material is due to ionised gas located in accretion disc winds or in biconical structures close to the nucleus (Malizia et al. 2012). A more complex interpretation pertains to those type 1 AGN that are hosted in edge-on galaxies and therefore fall within the bottom parts of panel c. First we notice that their number is limited, as expected on the basis of the consideration made in Sect. 4. These low numbers can either be due to a low probability of having a configuration with a face-on torus in an edge-on galaxy, or a high probability that absorbing material in a host galaxy viewed edge-on is sufficient to hide the BLR and to misclassify the object as a type 2 AGN. Since there is no reason why each of these possibilities is likely, it is possible that both concur to create the observed low number of type 1 AGN seen in edge-on galaxies. In particular we already know of type 1 AGN with absorbing material hosted in edge-on galaxies, which, however, is not high enough to hide the BLR. These are the objects located in the bottom left part of panel c; one of these AGN is IC 4329A where the presence of a dust lane observed in the equatorial plane of the host galaxy has been invoked to explain the source's mild X-ray neutral absorption, which, however, is below our limit of $N_{\rm H} = 4 \times 10^{21}$ cm^{-2} (Steenbrugge et al. 2005). The most particular objects are the three AGN, IGR J05347−6015, 4C +21.55, and ESO 140−G43, in the bottom right corner of the panel c. Although they have a column density Log$N_{\rm H} > 21.6$ and are hosted in low inclination angle galaxies, we still see their BLR. However, these objects are either poorly studied, as in the case of IGR J05347−6015 and 4C +21.55 (only *Swift*-XRT short observations were available to estimate the X-ray column density), or found to be absorbed by complex and ionised gas as for ESO 140−G43 (Ricci et al. 2010). In any case, given the uncertainty on the column density of these three objects, and given their proximity to the chosen b/a and Log$N_{\rm H}$ boundaries, no firm conclusion can be drawn.

In panel d of Fig. 7, the X-ray column density is plotted against the axial ratio of Seyfert 2 (black squares) and Seyfert 1.8−1.9 (blue squares) and, as for the type 1 AGN, open symbols indicate no intrinsic absorption or upper limits. In these objects the torus is by definition seen edge-on independently if the AGN is hosted in a face-on or an edge-on galaxy and they exhibit high absorption: hence these objects are expected to spread on the right side of the diagram over all values of b/a. Here the unusual objects are those found in the upper left corner of panel d; they have a column density too low to completely hide the BLR. Not considering Sey 1.8−1.9 types where an intrinsically variable ionising continuum or absorption/reddening unrelated to the torus can explain their intermediate classification, there are four objects: NGC 4736, IGR J19260+4136, IGR J03249+4041-SW, and IGR J14515−5542, optically classified as Seyfert 2, which have no absorption in X-rays. NGC 4736 is a nearby star-forming ring galaxy (van der Laan et al. 2015) where the torus is probably not present due to the low luminosity of the nucleus; star formation could then be responsible for the type 2 optical class. IGR J03249+4041-SW is one component of a pair of Seyfert 2 in close interaction (pair distance around 12 Kpc) and it is therefore possible that its type 2 class is simply due to dust associated with the galaxy merging. The other two AGN are poorly studied, but their column density is well measured and confirmed using XMM-INTEGRAL data for IGR J14515−5542 (De Rosa et al. 2012) and NuSTAR data for IGR J19260+4136 (our analysis) respectively. The fact that no prominent iron line is seen at soft X-ray energies excludes that these are Compton thick AGN (see Malizia et al. 2007); it is therefore very likely that they belong to the small fraction of naked Seyfert 2 galaxies where the torus is missing and the optical classification is due to other circumstances (Panessa & Bassani 2002). Otherwise they could

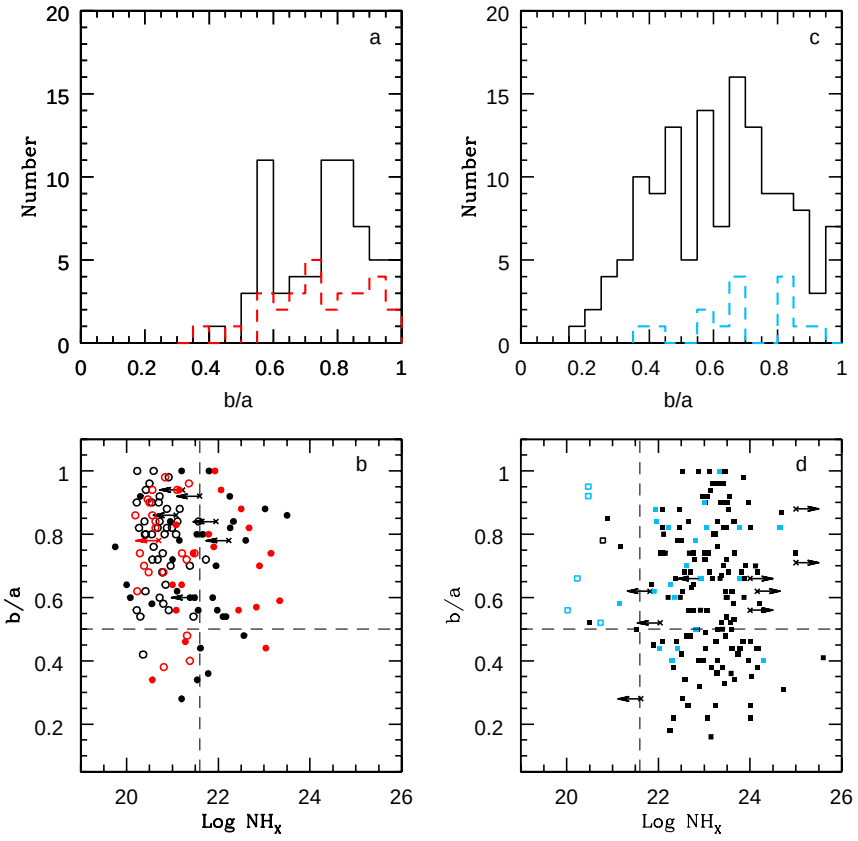

Fig. 7. Distributions of axial ratios and their relation with X-ray column density. *Upper panels*: distribution of host galaxy axial ratios. *Panel a*: Seyfert 1/1.2 (black line) and intermediate Seyfert 1.5 (red dashed line); *panel b*: Seyfert 2 (black line) and intermediate Seyfert 1.8/1.9 (blue dashed line). *Lower panels*: axial ratios versus X-ray absorption; *panel c*: broad line AGN (black circles Seyfert 1/1.2 and red circles Seyfert 1.5; *panel d*: narrow line AGN, black squares Seyfert 2 and blue squares Seyfert 1.8/1.9. Open circles refer to N_H upper limits or objects with no intrinsic absorption, i.e. only Galactic. Lines are as in Fig. 4.

be type 1 AGN where the combined effects of a very broadened emission profile and an intrinsic weakness with respect to the host galaxy conspire to produce a type 2 spectrum (Bianchi et al. 2019).

The objects in the bottom right corner Fig. 7d are the most relevant for the aim of this work. Following the scheme of Fig. 4, for these type 2 objects we cannot discriminate between absorption due to material located on large scales and related to the host galaxy, and that due to the torus.

6. Discussion

It is a well-known effect that optically selected type 1 Seyfert AGN tend to avoid edge-on host galaxies. Extensive studies have been performed in different wavebands in order to explain this bias (Keel 1980; Simcoe et al. 1997; Lagos et al. 2011) and although some objects missed in UV and optical surveys have been recovered going at higher energies, the deficit of type 1 hosted in edge-on galaxies still remains. A definitive test is that provided by the use of a hard X-ray selected sample that is less biased against obscured objects and therefore free from the limitation that affects surveys at other frequencies (i.e. from optical to soft X-rays). The first test at high energies was performed by Winter et al. (2009) on a limited *Swift*/BAT sample of around 80 AGN and also with this selection they found that edge-on galaxies only host the more absorbed AGN, finding that from the 11 edge-on sources in their sample, only one is associated with a Seyfert 1.

In this work using the INTEGRAL high energy selected sample of AGN (376 Seyferts), we have confirmed that there is a deficit of around 24% (±5%) of type 1 objects hosted in edge-on galaxies. Since this bias is not observational, that is, not due to the particular selection of the AGN sample, we deem that this effect is most likely physical and presumably due to the presence of absorption located in the large-scale structure of the host galaxy. This extra absorption, which we called for simplicity galactic, contributes to the total column density observed in X-rays and, even alone, could be sufficient to hide the broad line region providing a type 2 classification. The observed axial ratio distribution found in the present analysis can only be explained by considering a galactic absorption lying on the galaxy plane (e.g. inner bars, rings, dust lanes) in addition to the nuclear absorber.

In this picture, the role played by the orientation of the two absorbing structures (large and small scale) is obviously more complicated than in the more conventional unified picture where only the orientation of the torus determines if a source is classified as a type 1 or 2. Within this scenario either absorber is capable of attenuating the BLR flux, and so not only is the orientation of each with respect to the line of sight important but also their relative location and orientation. Following this scenario, when the torus and the galactic absorber are both edge-on, much of the absorbing material lies in the shadow of the torus leaving a wide range of angles that provide a direct view of the nucleus and therefore a type 1 classification. On the contrary, if the two absorbers are severely misaligned, then the absorbing material, either due to the torus or the galactic absorber, covers a much larger fraction of the nucleus, substantially increasing the probability that a randomly oriented observer will see a type 2 AGN. In this case we can have three configurations that provide a type 2 classification: one in which only the torus is detected, one where both absorbing structures lie along the line of sight and, finally, one where only a thick layer of galactic absorber is intercepted. In the first two cases the classification is that of a classical (torus hidden) type 2 AGN where the galactic absorption can eventually enhance the X-ray column density due to the torus. In

Table 1. Possible misclassified type 1.9/2 AGN.

Name	Dust [(†)]/Bar	Ref	NIR BLR	Ref
IGR J02343+3229 = NGC 973	DC/N	1	–	
IGR J09025−6814 = UGC 11397	–/Y	–	–	
NGC 2992	DC/N	2	Y	3
NGC 5506	D-S/Y	4	Y	5
NGC 5252	R-I/N	2	Y	5
IGR J19039+3344 = NGC 2788A	D/Y	6	–	
NGC 7172	DC/N	2	Y	7
NGC 7314	DC/Y	2	Y	5, 3
IGR J22367−1231 = MKN 915	DC/N	2	Y	5

Notes. [(†)]Same nomenclature as used by Malkan et al. (1998).
References. (1) Verstappen et al. (2013); (2) Malkan et al. (1998); (3) Onori et al. (2016); (4) Martini et al. (2003); (5) Lamperti et al. (2017); (6) NED; (7) Smajić et al. (2012).

the last case the source is formally not a type 2 AGN according to the classical unified theory, since the torus is not along the line of sight, but if Log$N_{\rm H}$ > 21.6 and the host galaxy is edge-on, the BLR becomes hidden and the source is optically classified as a type 2 AGN. In other words, if it were not for the host galaxy, these would be classified as type 1, meaning it is the host galaxy that makes them appear as type 2. Given their relevance, it is important to find some examples of these AGN within our large data-set. If we assumed that the parsec-scale tori are always Compton thick or nearly so (i.e. have column density above a few 10^{23} cm^{-2}), then objects with absorption much lower are probably hidden behind galactic material. Therefore in order to search for "misclassified" type 1 Seyferts, we focus on those Seyfert 1.8, 1.9, and 2 hosted in edge-on galaxies (i.e. with b/a below 0.5) and with mild X-ray absorption (below 10^{23} at cm^{-2}), which are those located in the dashed region of Fig. 4. There are 22 such objects in our sample of INTEGRAL AGN, most of which are newly discovered and therefore poorly studied. For nine of them broad band information could be gathered and analysed to verify their classification. These objects are shown in Table 1 where we list their name, presence of bar or dust lanes as reported in the literature, and evidence, from near infrared spectroscopy, of the presence of broad emission lines. The near infrared regime is particularly useful for this purpose since, being less affected by dust extinction, it is more likely to show a BLR that would be otherwise hidden in the optical band. The sources listed in Table 1 are clear examples of how a type 1 nucleus can hide behind absorbing structures that are located in the host galaxy. Some objects like NGC 7172 (Smajić et al. 2012), NGC 2992 (Trippe et al. 2008), NGC 5252 (Kotilainen & Prieto 1995), and NGC 5506 (Nagar et al. 2002) have already been discussed in the literature as examples of how a Seyfert 1 can be disguised as a Seyfert 2 due to galactic obscuration, while the other examples are suggested here for the first time. Although with the available observations their number is small (these objects represent 40% of the sample) and not yet sufficient to compensate for the lack of type 1 AGN in edge-on galaxies, their existence indicates this kind of *misclassification* due to galactic absorption can take place and, if extended to a large number of objects, might explain the difference in the axial ratio distributions of type 1 and 2 AGN. On the other hand, the existence of such objects gives support to the idea that an absorption located at larger scales is at work within a large fraction of local AGN.

Now that the co-evolution of galaxies and black holes is well established (e.g. see Heckman & Best 2014, and references therein) and ALMA observations are able to probe and image the gas within 100 pc of an AGN, evidence of multi-absorption components is beginning to accumulate. Mass and gas concentrations in host galaxies that are responsible for the feeding mechanism in AGN can also contribute to the obscuration of their nuclei. The mechanism appears to be that of kinematically decoupled embedded bars, which are the combination of a slowly rotating kiloparsec-scale stellar bar and a kinematically decoupled nuclear bar with overlapping dynamical resonances (Combes et al. 2013). Such resonances and kinematic decoupling are fostered by a large central mass concentration and high gas fraction. The gas is first halted in a nuclear ring (a few 100 pc in size), and then driven inwards under the influence of the decoupled nuclear bar obscuring the central engine. This has been observed in ESO 428−G14, where the measured kinematics is consistent with a nuclear inflow, or inner bar, which feeds the AGN (Feruglio et al. 2020).

Therefore the picture emerging from recent observations is that this galactic absorption may reside in different structures present in the host galaxy, which include dust lanes, bars and rings. In this paper we focus on their contribution to the obscuration of the direct radiation from the AGN especially when the host galaxy is seen edge-on. With this in mind Compton thick AGN could also be explained as sources in which the two absorbers on galactic and nuclear scales are both aligned and seen edge-on. A similar result was also obtained by Goulding et al. (2012), who studied the deep silicate absorption features seen in many Compton-thick AGN. Goulding et al. (2012) found that an important contribution to the observed mid-IR extinction in these objects is dust located in the host galaxy (i.e. it is due to disturbed morphologies, dust lanes, or galaxy inclination angles). However, these authors considered these two absorbers, galactic versus torus, as two alternative absorbing structures while here we assume that they could both be present in the same object and possibly aligned to enhance the nuclear obscuration. To produce Compton thick absorption our line of sight intercepts an edge-on torus and the galactic absorber (like for example an inner bar) can intervene or not depending on whether it is present or not in the host galaxy. The other possible geometry, that of a face on torus, either aligned or not with the galactic absorber, will always produce a Compton thin source (Buchner et al. 2019). Therefore we can say that a Compton thick AGN can have two types: one in which our line of sight intercepts only the torus and one in which both the torus and the galactic structure are seen edge-on. This last configuration produces objects like ESO 428−G14 and those discussed by Goulding et al. (2012). We note that the deep silicate absorption features observed in the Goulding et al. (2012) sample cannot be explained in terms of torus absorption models (see for example García-González et al. 2017) and can only be produced by dust on galactic scales.

7. Summary and conclusions

Using the hard X-ray selected sample of AGN detected by INTEGRAL/IBIS, in this work we have investigated the possible contribution of absorbing material located on a scale of hundreds of parsecs, that is, in the host galaxies, to the total amount of $N_{\rm H}$ measured in the X-ray band. By collecting the axial ratios (b/a) of the host galaxies for all our sample sources, we have verified that also within our hard X-ray selection sample there is a deficiency of around 24% (±5%) of type 1 AGN hosted in edge-on galaxies (those with b/a < 0.5). We have investigated the distribution of the host galaxy axial ratios in type 1 and type 2 AGN and further highlighted the optical Seyfert subclasses (type

1.5 for the unabsorbed and type 1.8 and 1.9 for absorbed AGN) to check whether there is a trend in the optical class with the inclination of the galaxy. In other words, we checked for the presence of absorption able to hide the BLR, or part of it, in the different galaxy axial ratios, and we found none. Possible bias in redshift has been excluded. We found the same effect in a well-determined range of z ($0.026 < z < 0.095$) where the number and the distributions of the two classes are statistically the same (at 99.9% confidence). Clearly this indicates that some material located in the host galaxy on scales of hundreds of parsecs and not aligned with the putative absorbing torus of the AGN can contribute to the column density measured in the X-ray band. In particular we have developed a scheme of the expected AGN type as a function of X-ray absorption and axial ratio in the different configuration of torus and galaxy inclinations: when the torus is seen edge-on, we always have a type 2 absorbed AGN independently of the host galaxy orientation; when the torus is seen face-on, we may have a type 1 AGN unabsorbed or mildly absorbed, or misclassified type 2 objects where the absorption is on galactic scales. Plotting the axial ratio versus the column density for type 1 and type 2, we have highlighted peculiar sources and in particular have been able to identify a set of possible misclassified type 2 AGN, which are absorbed (type 2) and located in edge-on galaxies. Our conclusion is that these absorptions, galactic versus torus, are not alternative but could be both present in the same object and possibly aligned to enhance the nuclear obscuration. Within this scenario a Compton thick AGN can be explained by two formats: one in which our line of sight intercepts only the torus and one in which both the torus and the galactic structure are seen edge-on.

Acknowledgements. The authors acknowledge financial support from Agenzia Spaziale Italiana under contract no. 2019-35-HH.0. We acknowledge the use of the HyperLeda database (http://leda.univ-lyon1.fr). This research has made use of the NASA/IPAC Extragalactic Database (NED) and NASA/IPAC Infrared Science Archive, which are operated by the Jet Propulsion Laboratory, California Institute of Technology, under contract with the National Aeronautics and Space Administration. Acknowledgements go to Rick White at Pan-STARRS database for his help in finding and interpreting PS1 tables. We thank Chiara Feruglio for worthwhile discussion. The authors also thank Marco Mignoli for useful discussions on AGN and host galaxy characteristics in the optical/IR band, and Eliana Palazzi and Andrea Rossi for imaging analysis in the optical/IR band. We thank the anonymous referee for useful remarks that helped us to improve the quality of this paper.

References

Antonucci, R. 1993, ARA&A, 31, 473
Bianchi, S., Maiolino, R., & Risaliti, G. 2012, Adv. Astron., 2012, 1
Bianchi, S., Antonucci, R., Capetti, A., et al. 2019, MNRAS, 488, L1
Bird, A. J., Bazzano, A., Malizia, A., et al. 2016, ApJS, 223, 15
Brightman, M., & Nandra, K. 2011, MNRAS, 413, 1206
Buchner, J., Brightman, M., Nandra, K., Nikutta, R., & Bauer, F. E. 2019, A&A, 629, A16
Cappi, M., Panessa, F., Bassani, L., et al. 2006, A&A, 446, 459
Chambers, K. C., Magnier, E. A., Metcalfe, N., et al. 2016, ArXiv e-prints [arXiv:1612.05560]
Combes, F., García-Burillo, S., Casasola, V., et al. 2013, A&A, 558, A124
Combes, F., García-Burillo, S., Audibert, A., et al. 2019, A&A, 623, A79
De Rosa, A., Panessa, F., Bassani, L., et al. 2012, MNRAS, 420, 2087
de Vaucouleurs, G. 1959, Handb. Phys., 53, 275
Di Gesu, L., Costantini, E., Piconcelli, E., et al. 2014, A&A, 563, A95
Elitzur, M. 2008, New Astron. Rev., 52, 274
Ferruit, P., Wilson, A. S., & Mulchaey, J. 2000, ApJS, 128, 139
Feruglio, C., Fabbiano, G., Bischetti, M., et al. 2020, ApJ, 890, 29
García-Burillo, S., Combes, F., Schinnerer, E., Boone, F., & Hunt, L. K. 2005, A&A, 441, 1011
García-Burillo, S., Combes, F., Usero, A., et al. 2014, A&A, 567, A125
García-González, J., Alonso-Herrero, A., Hönig, S. F., et al. 2017, MNRAS, 470, 2578
Gelbord, J. M., Weaver, K. A., & Yaqoob, T. 2006, in The X-ray Universe 2005, ed. A. Wilson, ESA Spec. Publ., 604, 619
González-Martín, O., Masegosa, J., Márquez, I., Guerrero, M. A., & Dultzin-Hacyan, D. 2006, A&A, 460, 45
Goulding, A. D., Alexander, D. M., Bauer, F. E., et al. 2012, ApJ, 755, 5
Heckman, T. M., & Best, P. N. 2014, ARA&A, 52, 589
Hickox, R. C., & Alexander, D. M. 2018, ARA&A, 56, 625
Hirashita, H., & Nozawa, T. 2017, Planet. Space Sci., 149, 45
Hönig, S. F. 2019, ApJ, 884, 171
Hönig, S. F., & Kishimoto, M. 2017, ApJ, 838, L20
Hubble, E. P. 1926, ApJ, 64, 321
Huchra, J. P., Macri, L. M., Masters, K. L., et al. 2012, ApJS, 199, 26
Jarrett, T. H., Chester, T., Cutri, R., Schneider, S. E., & Huchra, J. P. 2003, AJ, 125, 525
Keel, W. C. 1980, AJ, 85, 198
Kocevski, D. D., Brightman, M., Nandra, K., et al. 2015, ApJ, 814, 104
Koss, M., Mushotzky, R., Veilleux, S., & Winter, L. 2010, ApJ, 716, L125
Kotilainen, J. K., & Prieto, M. A. 1995, A&A, 295, 646
Krivonos, R. A., Tsygankov, S. S., Mereminskiy, I. A., et al. 2017, MNRAS, 470, 512
Lagos, C. D. P., Padilla, N. D., Strauss, M. A., Cora, S. A., & Hao, L. 2011, MNRAS, 414, 2148
Lamperti, I., Koss, M., Trakhtenbrot, B., et al. 2017, MNRAS, 467, 540
Madrid, J. P., Chiaberge, M., Floyd, D., et al. 2006, ApJS, 164, 307
Maia, M. A. G., Machado, R. S., & Willmer, C. N. A. 2003, Bull. Astron. Soc. Braz., 23, 156
Maiolino, R., & Rieke, G. H. 1995, ApJ, 454, 95
Maiolino, R., Risaliti, G., & Salvati, M. 1999, A&A, 341, L35
Makarov, D., Prugniel, P., Terekhova, N., Courtois, H., & Vauglin, I. 2014, A&A, 570, A13
Malizia, A., Landi, R., Bassani, L., et al. 2007, ApJ, 668, 81
Malizia, A., Stephen, J. B., Bassani, L., et al. 2009, MNRAS, 399, 944
Malizia, A., Bassani, L., Bazzano, A., et al. 2012, MNRAS, 426, 1750
Malizia, A., Landi, R., Molina, M., et al. 2016, MNRAS, 460, 19
Malkan, M. A., Gorjian, V., & Tam, R. 1998, ApJS, 117, 25
Martini, P., Regan, M. W., Mulchaey, J. S., & Pogge, R. W. 2003, ApJS, 146, 353
Mateos, S., Carrera, F. J., Alonso-Herrero, A., et al. 2016, ApJ, 819, 166
Matt, G. 2000, A&A, 355, L31
McKernan, B., Ford, K. E. S., & Reynolds, C. S. 2010, MNRAS, 407, 2399
Mereminskiy, I. A., Krivonos, R. A., Lutovinov, A. A., et al. 2016, MNRAS, 459, 140
Miniutti, G., Piconcelli, E., Bianchi, S., Vignali, C., & Bozzo, E. 2010, MNRAS, 401, 1315
Molina, M., Bassani, L., Malizia, A., et al. 2013, MNRAS, 433, 1687
Nagar, N. M., Oliva, E., Marconi, A., & Maiolino, R. 2002, A&A, 391, L21
Oda, S., Tanimoto, A., Ueda, Y., et al. 2017, ApJ, 835, 179
Onori, F., La Franca, F., Ricci, F., et al. 2016, MNRAS, 464, 1783
Panessa, F., & Bassani, L. 2002, A&A, 394, 435
Panessa, F., Bassani, L., Landi, R., et al. 2016, MNRAS, 461, 3153
Patrick, A. R., Reeves, J. N., Porquet, D., et al. 2012, MNRAS, 426, 2522
Prieto, M. A., Mezcua, M., Fernández-Ontiveros, J. A., & Schartmann, M. 2014, MNRAS, 442, 2145
Ricci, C., Beckmann, V., Audard, M., & Courvoisier, T. J.-L. 2010, A&A, 518, A47
Ricci, C., Trakhtenbrot, B., Koss, M. J., et al. 2017, ApJS, 233, 17
Sazonov, S., Churazov, E., & Krivonos, R. 2015, MNRAS, 454, 1202
Schinnerer, E., Eckart, A., & Tacconi, L. J. 1999, ApJ, 524, L5
Simcoe, R., McLeod, K. K., Schachter, J., & Elvis, M. 1997, ApJ, 489, 615
Smajić, S., Fischer, S., Zuther, J., & Eckart, A. 2012, A&A, 544, A105
Steenbrugge, K. C., Kaastra, J. S., Sako, M., et al. 2005, A&A, 432, 453
Trippe, M. L., Crenshaw, D. M., Deo, R., & Dietrich, M. 2008, AJ, 135, 2048
Trippe, M. L., Crenshaw, D. M., Deo, R. P., et al. 2010, ApJ, 725, 1749
Tsvetanov, Z., Caganoff, S., Kriss, G. A., et al. 1992, in American Astronomical Society Meeting Abstracts #180, BAAS, 24, 752
Urry, C. M., & Padovani, P. 1995, PASP, 107, 803
Ursini, F., Bassani, L., Panessa, F., et al. 2017, MNRAS, 474, 5684
van der Laan, T. P. R., Armus, L., Beirao, P., et al. 2015, A&A, 575, A83
Vasudevan, R. V., Brandt, W. N., Mushotzky, R. F., et al. 2013, ApJ, 763, 111
Verstappen, J., Fritz, J., Baes, M., et al. 2013, A&A, 556, A54
Winter, L. M., Mushotzky, R. F., Reynolds, C. S., & Tueller, J. 2009, ApJ, 690, 1322

Appendix A: New INTEGRAL AGN

Here we discuss the new AGN reported by Mereminskiy et al. (2016) in deep extragalactic surveys, and those reported by Krivonos et al. (2017) from an extensive galactic plane mapping. Amongst the 147 sources reported by Mereminskiy et al. (2016), 70 are new hard X-ray emitting objects that have never been reported in previous INTEGRAL surveys (Bird et al. 2016, and references therein): 23 of these are still unidentified and therefore have not been considered. Of the remaining 47 objects, all optically classified as AGN, eight are blazars and seven have no X-ray observation available to characterise their 2−10 keV spectra; they have therefore been excluded from the list of AGN considered in this work. The remaining 33 objects have instead been added to the large database of INTEGRAL AGN (Malizia et al. 2012, 2016). Regarding instead the new hard X-ray sources reported in the Galactic Plane Survey by Krivonos et al. (2017), 21 are identified with AGN by the authors: 11 are unambiguously classified as Seyfert galaxies and therefore have been added to the INTGRAL AGN sample, while the rest, being either blazars or objects of unknown class, have been omitted. All these new entries (33 + 11) have been listed in Tables A.2 and A.3 together with their coordinates, redshift, optical class, and X-ray spectral parameters (column density, photon index, 2−10 and 20−100 keV fluxes) for uniformity with the work of Malizia et al. (2012, 2016). It is worth noting that these new additions have also been unambiguously associated with their X-ray counterparts thus allowing us to restrict their positional error box and therefore to optically identify and classify them with good confidence. To provide the X-ray spectral parameters for these 44 new AGN, we have checked both the literature and the archives to search for information. In many cases, the X-ray data analysis has already been performed and the results reported in various publications as listed in the last column of Tables A.2 and A.3. For seven objects the X-ray data analysis is performed and presented here using archival *Swift*/XRT observations; in a couple of cases we preferred to re-analyse the data since more exposure or unconvincing results were found (e.g. IGR J21099+3533 and IGR J21382+3204 already analysed by Ricci et al. 2017). The 2−10 keV spectral analysis has been performed following the method described in Malizia et al. (2016); the 20−100 keV fluxes have been converted from the 17−60 keV flux reported in Mereminskiy et al. (2016) and Krivonos et al. (2017) by assuming a simple power law $\Gamma = 2.01 \pm 0.04$, as found by Molina et al. (2013).